Liquid Crystals
Publication details, including instructions for authors and subscription information:
http://www.informaworld.com/smpp/title~content=t713926090

Quasi-mesoscopic model for ferroelectric switching in the chevron geometry

L. D. Hazelwood[a]; T. J. Sluckin Corresponding author[a]
[a] School of Mathematics, University of Southampton, Highfield, Southampton SO17 1BJ, UK

Online publication date: 25 May 2010

To cite this Article Hazelwood, L. D. and Sluckin Corresponding author, T. J.(2004) 'Quasi-mesoscopic model for ferroelectric switching in the chevron geometry', Liquid Crystals, 31: 5, 683 — 695
To link to this Article: DOI: 10.1080/02678290410001670601
URL: http://dx.doi.org/10.1080/02678290410001670601

LIQUID CRYSTALS, VOL. 31, NO. 5, MAY 2004, 683–695

Taylor & Francis
Taylor & Francis Group

Quasi-mesoscopic model for ferroelectric switching in the chevron geometry

L. D. HAZELWOOD and T. J. SLUCKIN*
School of Mathematics, University of Southampton, Highfield, Southampton SO17 1BJ, UK

(*Received 26 August 2003; accepted 16 January 2004*)

We present a theory of ferroelectric liquid crystal switching which combines elements of standard macroscopic continuum theories with mesoscopic Landau–de Gennes chevron theories. The macroscopic elements of the theory apply in the chevron arms, and are subject to a boundary condition at the chevron interface. This boundary condition can be derived from an anchoring energy associated with the director discontinuity at the chevron tip. The anchoring energy, which corresponds to the degree to which the cone mismatch condition is not satisfied, is calculated using the mesoscopic Landau–de Gennes theory. In the combined theory the frequently used cone-matching condition emerges as a thick cell limit. We are able to calculate a free energy associated with the imposition of a field on particular configurations. There follows a switching phase diagram determining the conditions for thresholdless and bistable switching. We further show that the time dependence of the switching process is determined by the slower bulk relaxation dynamics rather than by the fast chevron surface dynamics.

1. Introduction

The intrinsic chiral nature of the smectic C* phase has the physical consequence that it induces a spontaneous polarization, on symmetry grounds, as suggested by Meyer *et al.* [1] and thus the smectic C* is naturally ferroelectric. The first application of ferroelectric liquid crystals to display devices was due to Clark and Lagerwall [2]. Devices involving a ferroelectric liquid crystal were observed to possess the following properties: (a) fast switching times due to linear coupling between the spontaneous polarization and the applied electric field; (b) the interaction with the cell surface can act to unwind the natural ferroelectric helix; (c) the formation of domains of differing polarizations separated by domain walls; and (d) a threshold voltage necessary for switching to occur. This strong influence of the surface in these devices has given rise to their common name: surface stabilized ferroelectric liquid crystals (SSFLCs).

The first attempt to model SSFLC devices using a continuum Frank–Oseen-type formulation was by Handschy and Clark [3]. Their simple model was sufficient to explain the observed helical unwinding, the development of polarization domains and to provide some switching dynamics. They assumed that the ferroelectric arranged itself into a planar arrangement of smectic layers, referred to as the bookshelf geometry (see figure 1 (*a*)). However, Rieker *et al.* [4] experimentally found this structure to be more frequently replaced by the more complex chevron structure, as shown in figure 2 (*a*). This structure possesses large regions of uniformly tilted layers (chevron arms), together with very narrow regions of rapidly changing orientation in the middle of the cell (the chevron tip) as well as close to the cell boundaries. However, the existence of chevrons provides technical advantages following from the possibility of bistable switching, as well as interesting physical modelling opportunities.

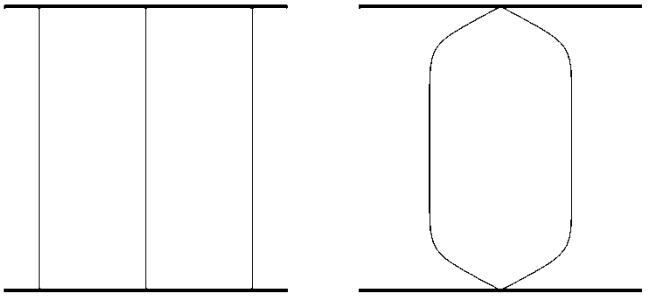

Figure 1. Bookshelf (side view) and up/down director configurations of switched states (end view).

*Author for correspondence; e-mail: t.j.sluckin@soton.ac.uk

Liquid Crystals ISSN 0267-8292 print/ISSN 1366-5855 online © 2004 Taylor & Francis Ltd
http://www.tandf.co.uk/journals
DOI: 10.1080/02678290410001670601

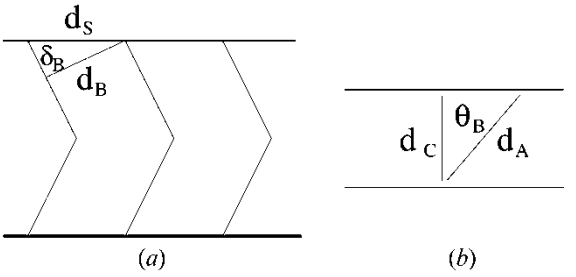

Figure 2. Chevron structure and layer thicknesses.

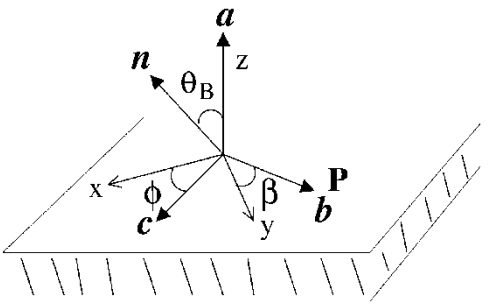

Figure 3. Vector coordinate system for smectic C* phase.

The development of models to describe ferroelectric switching has proven difficult. This is largely due to the contrasting length scales associated with the chevron arms and tip. In the arms, the molecular alignment changes slowly, making macroscopic continuum theories, such as the smectic C elastic continuum theory developed by Leslie *et al.* [5], the ideal tool for investigating the switching process. However, these theories fail to incorporate the physics necessary to describe molecular changes that occur on the chevron interface length scale. At these lengths phenomenological Landau–de Gennes-type theories are more appropriate, but become computationally expensive when applied to the SSFLC device dimensions. Vaupotič *et al.* [6] have demonstrated that studies on relatively thin cells are possible using this approach. An alternative approach has been to produce a hybrid model. This uses a macroscopic model in the chevron arms (regions of uniform tilt), but replaces the chevron interface by an *ad hoc* torque condition (Maclennan *et al.* [7, 8] and Ulrich and Elston [9]) or by a critical torque threshold (Brown *et al.* [10]). Both of these hybrid models lead to the explicit inclusion of a finite field switching threshold.

In this paper we unify these two theoretical approaches. We build on previous work [7–10] and provide a calculational framework for investigating ferroelectric switching, explicitly including the chevron interface physics. We show that it is possible to obtain an analytical expression for the chevron interface energy provided we make some plausible physical assumptions. This interfacial energy condition will allow us to formally derive the chevron interface matching, or cone matching, condition. A natural corollary of this result is that it is possible to construct a switching phase diagram, defining parameter regimes for thresholdless and bistable switching.

The paper is organized as follows. In § 2 some basic ferroelectric physics and modelling will be introduced. A description of our extended hybrid model will also be described. Section 3 derives the chevron interface surface tension. In § 4 we derive the cone matching condition and present the switching phase diagram. Section 5 describes the dynamical extension to this model, where key features and some numerical results are presented. Finally, § 6 discusses and concludes the paper.

2. Basic modelling and notation

2.1. *Smectic C* phase*

Ferroelectric smectic C* liquid crystals tend to organize themselves into layers in which the molecular director **n** is tilted away from the layer normal **a** by the so-called smectic cone angle θ_B, shown in figure 3. The projection of the director onto the smectic planes is often denoted as the *c*-director in continuum modelling. The intrinsic chirality of these molecules leads to a helical precession of the molecules in the direction of the layer normal. This symmetry condition enables an external field to induce a spontaneous polarization **P**. This spontaneous polarization is oriented in the direction $\mathbf{b} = \mathbf{a} \times \mathbf{c}$.

The coupling of the electric field with the polarization leads to a reduction in the electrical energy density [11]:

$$f_p = -\mathbf{P}\cdot\mathbf{E}. \tag{1}$$

This field coupling is the main mechanism for low field switching in ferroelectric cells. In the high field limit the switching process is additionally influenced by nonlinear dielectric contributions.

2.2. *Device physics and chevron geometry*

Clark and Lagerwall [2] found that when FLCs are placed within an LC cell the interaction of the surface tends to unwind the natural helix, with the bulk adopting an almost homogeneous alignment set by the cell surface. Handschy and Clark developed a switching model capable of predicting up and down polarization domains depending on the direction of **E**. They assumed the bookshelf geometry for their calculations.

However, Rieker *et al.* [4] demonstrated that this bookshelf structure is often replaced by the so-called

chevron structure. The crucial idea behind the chevron structure is that the layer tilt arises because of a mismatch between the natural thermodynamically stable smectic layer thickness in the bulk (d_B) and the layer thickness imposed by the layer pinning at the cell surface (d_S). Limat and Prost [12] have associated a layer strain $\varepsilon = d_S/d_B - 1$ as a measure of the layer thickness mismatch. The strain imposed by the surface can be minimized by rotating the layers through a tilt angle $\delta_B = \cos^{-1}(d_B/d_S)$, as shown in figure 2. The layer tilt permits the layers not to pay the energetic price of dilatation.

However the countervailing consequence is that three narrow regions of drastic reorientation are inserted. Two of these regions are located close to the cell surfaces, but one is in the centre of the cell. This region is often known as the chevron interface. In the transition regions there is a balance between compression and curvature energies. In addition the surface regions include extra complications through complex and still relatively unknown surface interactions.

Layer thinning is the driving mechanism of chevron formation in both smectic A and smectic C liquid crystal phases. There are, however, some differences in the underlying physics of these two related phenomena. In the smectic A phase the layers simply undergo a small degree of layer thinning on cooling. By contrast, in the smectic C phase the layer thinning is primarily a result of molecular tilt occurring at the smectic A to smectic C phase transition. This thickness change defines the smectic C cone angle through $\theta_B = \cos^{-1}(d_C/d_A)$, and is shown in figure 2 (*b*). Theories describing the formation of chevrons in the smectic A phase have been presented by Limat and Prost [12], and in more detail, using a Landau–de Gennes free energy formulation, by Kralj and Sluckin [13]. More recently an analogous theory for smectic C chevrons has been put forward by Vaupotič *et al.* [14].

2.3. *Chevron interface and the cone matching condition*

In order to understand switching in ferroelectrics it is necessary to understand the behaviour of the director across the chevron interface. This is a somewhat complex problem, requiring a full solution of the Landau–de Gennes smectic C theory [14]. However, it is possible to make some progress because the chevron interface thickness λ is small in comparison to the length over which electric distortions relax ξ. Clark and Rieker [15] have suggested that, because λ is extremely sharp, the chevron interface may effectively be regarded as a discontinuous surface boundary when investigating the ferroelectric switching process for macroscopic theories. If one enforces this discontinuous boundary, it is possible to generate three geometrical scenarios in terms of layer tilt angle δ_B and smectic C cone angle θ_B:

(1) $\theta_B > \delta_B$. There is an overlap between the cones at the interface, and thus it is possible to maintain continuity of the nematic director field. This is known as the cone matching condition, and is shown in figure 4. This leads geometrically to two important angular quantities for modelling purposes. The first is the rotational angle at the discontinuity ϕ_c, defined relative to the x-direction in the tilted layer reference frame. The second is the angular component α_c in the y-direction at the discontinuity. We will refer to this simply as the out-of-plane director tilt. This is a requirement for bistable ferroelectric switching. Using the coordinate system shown in figure 4 it is straightforward to show ϕ_c and α_c are defined respectively by

$$\phi_c = \cos^{-1}\left(\frac{-\tan\delta_B}{\tan\theta_B}\right)$$
$$\alpha_c = \cos^{-1}\left(\frac{\cos\theta_B}{\cos\delta_B}\right). \tag{2}$$

Rieker *et al.* [4] observed experimentally the following angular relation

$$\delta_B^2 = \theta_B^2 - \alpha_c^2. \tag{3}$$

(2) $\theta_B = \delta_B$. This case is the limit of the first scenario, for which the smectic cones only just touch at the interface. There is no out-of-plane director tilt and no possibility for bistable switching.

(3) $\theta_B < \delta_B$. This case is forbidden geometrically as there is no way to maintain director continuity across the interface.

2.4. *Macroscopic continuum modelling*

The standard continuum modelling formulation, derived by Leslie *et al.* [5], is written as

$$\begin{aligned} 2f_B = {} & A_{12}(\mathbf{b}\cdot\nabla\times\mathbf{c})^2 + A_{21}(\mathbf{c}\cdot\nabla\times\mathbf{b})^2 \\ & + 2A_{11}(\mathbf{b}\cdot\nabla\times\mathbf{c})^2(\mathbf{c}\cdot\nabla\times\mathbf{b})^2 \\ & + B_1(\nabla\cdot\mathbf{b})^2 + B_2(\nabla\cdot\mathbf{c})^2 \\ & + \frac{1}{4}B_3[\mathbf{b}\cdot(\nabla\times\mathbf{b}) + \mathbf{c}\cdot(\nabla\times\mathbf{c})]^2 \\ & + B_{13}(\nabla\cdot\mathbf{b})[\mathbf{b}\cdot(\nabla\times\mathbf{b}) + \mathbf{c}\cdot(\nabla\times\mathbf{c})] \\ & + 2C_1(\nabla\cdot\mathbf{c})(\mathbf{b}\cdot\nabla\times\mathbf{c}) + 2C_2(\nabla\cdot\mathbf{c})(\mathbf{c}\cdot\nabla\times\mathbf{b}) \end{aligned} \tag{4}$$

where A_{ij}, B_i and C_i are the smectic C elastic constants

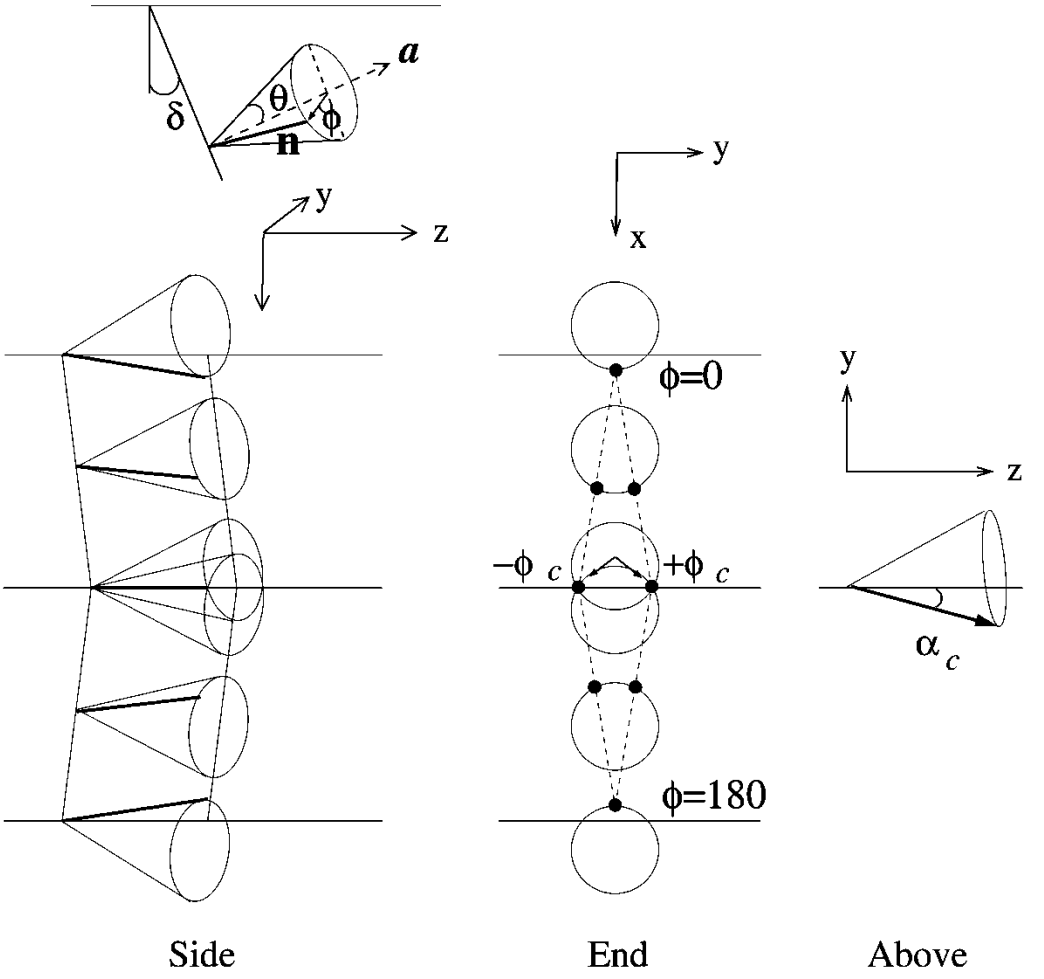

Figure 4. Cone matching and director profiles. The top picture shows the smectic C cone in a space-fixed set of axes, and shows the possible equilibrium directors consistent with a given layer orientation. The picture marked 'Side' gives a side view of how this cone changes across the cell, as the layer direction changes more or less discontinuously at the chevron interface. That marked 'End' shows the same phenomenon, now viewed by an observer looking down the cell and able to see azimuthal changes. The picture marked 'Above' shows the out-of-plane director tilt α_c at the chevron interface.

as defined in [5]. Matching these elastic constants with experimental results has proven extremely successful [10].

However, in this formulation layer shrinkage (or equivalently changes in smectic cone angle) has not been taken into account. It is thus not possible to describe the chevron structure. Other more complex formulations that include layer compression have been presented by Nakagawa [16], de Meyere and Dahl [11] and Sabater *et al.* [17] but have been used less frequently in the identification of ferroelectric material parameters. It is, however, well suited to describing director deformation in uniformly tilted regions such as the chevron arms. In this case the free energy can be written, together with the contribution due to the ferroelectric polarization, equation (1), as

$$F = \int_0^L [f_b + f_p + f_d]\,dx \tag{5a}$$

$$f_b = \Big\{ B_1(\nabla\cdot\mathbf{b})^2 + B_2(\nabla\cdot\mathbf{c})^2 + \frac{1}{4}B_3[\mathbf{b}\cdot(\nabla\times\mathbf{b}) + \mathbf{c}\cdot(\nabla\times\mathbf{c})]^2, + B_{13}(\nabla\cdot\mathbf{b})[\mathbf{b}\cdot(\nabla\times\mathbf{b}) + \mathbf{c}\cdot(\nabla\times\mathbf{c})] \Big\} \tag{5b}$$

$$f_p = -\mathbf{P}\cdot\mathbf{E}. \tag{5c}$$

2.5. *Mesoscopic Landau–de Gennes modelling*

In a Landau-de Gennes formulation the free energy is based upon an expansion of phenomenological terms using the relevant smectic C phase order parameters.

The free energy is determined in terms of the regular director field $\mathbf{n}(\mathbf{r})$ but with the addition of a complex smectic order parameter $\Psi(\mathbf{r})$. This additional order parameter includes the degree of layer order η and the position of the layers through a phase function W:

$$\Psi(\mathbf{r}) = \eta(\mathbf{r}) \exp[\mathrm{i} W(\mathbf{r})]. \tag{6}$$

In the case of chevrons the phase function describes a distortion $u(\mathbf{r})$ away from a homogeneous bookshelf configuration. The phase function W is thus written

$$W(\mathbf{r}) = q[z - u(\mathbf{r})] \tag{7}$$

where $q = 2\pi/d$ is an imposed surface layer periodicity. This can also be thought of as a far field bulk layer spacing condition that can be used to determine the layer tilt angle $\delta_B = \cos^{-1}(q/q_B)$. The director is defined using the coordinate system shown in figure 4 to be

$$\begin{aligned}\mathbf{n} = (&\sin\theta\cos\phi\cos\delta + \sin\delta\cos\theta,\ \sin\theta\sin\phi,\\ &\cos\theta\cos\delta - \sin\delta\sin\theta\cos\phi).\end{aligned} \tag{8}$$

The construction of a free energy to describe distortions of the director and complex smectic order parameter is not trivial, as any formulation must respect the smectic C symmetries. In this paper we shall use a smectic C phenomenological theory, similar to that used by Vaupotič *et al.* [14] in the study of smectic C chevrons. The free energy is written as

$$\mathcal{F} = \int_V [f_N + f_A + f_C] \mathrm{d}^3\mathbf{r} \tag{9a}$$

$$f_N = \frac{1}{2}K_1(\nabla\cdot\mathbf{n})^2 + \frac{1}{2}K_2(\mathbf{n}\cdot\nabla\times\mathbf{n})^2 + \frac{1}{2}K_3(\mathbf{n}\times\nabla\times\mathbf{n})^2 \tag{9b}$$

$$f_A = \frac{1}{2}\gamma_{\|}|(\mathbf{n}\cdot\nabla - \mathrm{i}q_A)\psi|^2 + \frac{1}{2}\gamma_{\perp}|(\mathbf{n}\times\nabla)\psi|^2 \tag{9c}$$

$$f_C = \frac{1}{2}D_{\perp}|\nabla_{\perp}^2\psi|^2. \tag{9d}$$

Here f_N is the usual Frank nematic energy describing splay, twist and bend deformation. f_A is the smectic A contribution composed of a dilatational energy term ($\gamma_{\|}$) and smectic A stabilizing term ($\gamma_{\perp}$). For $\gamma_{\perp} > 0$ the molecules are constrained energetically to lie along the layer normal, i.e. smectic A phase. By contrast, on cooling into the smectic C phase the molecules are allowed to tilt away from the layer normal, achieved by setting $\gamma_{\perp} < 0$. In order to prevent the molecules tilting too far, a smectic C stabilizing term f_C is required. This term allows the existence of finite cone angle and maintains layer continuity [18].†

This type of theory provides an ideal framework for investigating transition regions such as the chevron tip and cell surfaces. However, the continuum theory is more appropriate in slowly changing regions such as the chevron arms.

2.6. *Hybrid switching model*

We now introduce a hybrid model of ferroelectric switching that combines the simplicity of the macroscopic switching model with a mesoscopic model of the chevron tip. The hybrid model essentially involves three components:

(1) In the chevron arms we use the macroscopic smectic C continuum model given by equation (5*a*). The geometry of the chevron arms enables the free energy to be expressed in terms of a single rotation variable ϕ. This rotational value matches up to a chevron surface boundary condition $\phi = \phi_S$, determined by the mesoscopic calculation.

(2) In the transition region or chevron interface, the mesoscopic Landau–de Gennes formulation is used to calculate a surface tension or surface energy as a function of ϕ_S. This calculation is presented in § 3.

(3) We construct dynamic switching equations that incorporate both the bulk and chevron surface switching. The dynamics of the bulk are governed by the field which induces spontaneous polarization, macroscopic elastic distortion, bulk viscosity and the chevron surface condition, $\phi = \phi_S$. Neglecting backflow we write the dynamics in terms of a time-dependent Ginzburg–Landau equation for the both the bulk, $\phi(x, t)$, and the surface $\phi_S(t)$. The relaxation times are governed by the material viscosities of the bulk and the surface. The calculations for the static solutions are presented in § 4, and those for the dynamical solutions in § 5.

In order to simplify the complexity of the calculation, the following assumptions have been made:

(a) Only a symmetric chevron that is homogeneous in the y- and z-directions will be considered, and so $\mathbf{n} = \mathbf{n}(x)$ and $W = q[z - u(x)]$. The symmetry enables a reduction in the calculation to half

†This term is different from the original Vaupotič *et al.* [14] ($D|(n\times\nabla)^2\Phi|^2$) formulation and has been proposed by Chen and Lubensky, where $\nabla_{\perp}^2 = (\delta_{ij} - n_i n_j)\nabla_i\nabla_j$. In the level of approximation to be used here it would have made little difference to the results using either formulation, and would have only served to complicate the calculations.

of a cell, greatly simplifying the mesoscopic chevron surface calculation.

(b) The ferroelectric coupling of polarization is only included in the chevron arms, where the macroscopic continuum theory is easily applied. In principle, this coupling should also be included in the chevron surface term. In practice, this chevron region is small and is expected to make only a small contribution to the director torque due to the tip.

(c) The electric field is assumed to be uniform through the cell ($E(\mathbf{r})=[E, 0, 0]$). While it is clear that it is the D-field that is conserved within ferroelectric cells it requires a self-consistent calculation of the director configuration and the field. In principle, a fully self-consistent calculation is possible (see, for example, Brown *et al.* [10] and de Meyere and Dahl [11]). However, in practice, the effect is not expected to alter the generic structure of the switching phase diagram and will therefore not be included here.

(d) We use the nematic one-elastic constant approximation within the mesoscopic calculation, $K=K_i$ for $i=1, 2, 3$.

3. Chevron interfacial energy

In this section we calculate a surface energy $w(\phi_s)$ using the Landau–de Gennes smectic C theory discussed in § 2. This methodology is similar to that used in the calculation of smectic A chevron interface boundaries. However, in that case Limat and Prost [12] have shown that the underlying phenomenological terms can be integrated to provide a surface energy as a function of equilibrium tilt angle δ_E of the boundary. The new feature in the present model is that δ will be replaced by the rotational angle ϕ_s, which is prescribed as the far field boundary condition.

In order to derive the surface energy condition it will be necessary to separate the derivation into three parts, and described in the following subsections. In the first part we will use the dominance of the dilatational thermodynamical force to enable us to re-write the original formulation in a more physically intuitive way. This will lead to the easy identification of equilibrium quantities such as the smectic C cone angle and the out-of-plane director tilt. In the second part, we enforce the smectic C dilatational energy to be minimized everywhere. This allows an explicit calculation of the equilibrium static layer profile. In the third part we finally calculate the free energy of the interface by quasi-statically changing ϕ_S, using the equilibrium layer profile derived earlier in the second part.

3.1. *Preliminaries and equilibrium properties*

In the far field, away from the chevron tip, the layers show uniform tilt. This will be the same as unconstrained equilibrium, in which the layers possess zero layer dilatation and the molecules lie at a constant angle relative to the smectic C layers. We can define a zero dilatation condition upon setting equation (9 *c*) to zero:

$$[(\mathbf{n}\cdot\nabla W_e)-q_A]=0. \tag{10}$$

We will now use this condition to obtain an angular relation between layer tilt angle δ, the equilibrium cone angle θ_B and the degree of out-of-plane director tilt α_c in terms of phenomenological parameters. We substitute for n, W and zero dilatation, equations (7), (8) and (10), and inserting the approximation $\delta\approx-\mathrm{d}u/\mathrm{d}x$ enables equation (10) in the limit of small angles to be written:

$$\left[\delta^2-\theta^2-2\varepsilon\right]=0. \tag{11}$$

Notice that we have identified the layer strain $\varepsilon=1-q_s/q_A$. δ and θ are related to each other through a layer thickness mismatch. There are three scenarios relating δ and θ in terms of the layer strain ε. With $\varepsilon=0$ ($d_A=d_S$) then the smectic cone angle is equal to the layer tilt, $\theta=\delta$. With $\varepsilon>0$ ($d_A<d_S$) the smectic cone angle is less the layer tilt, $\theta<\delta$. The third possibility is when $\varepsilon<0$ ($d_A>d_S$) the smectic cone angle is greater than the layer tilt, $\theta>\delta$. This is the case found experimentally.

Interestingly, it is this case that must be satisfied to produce out-of-plane director tilt at the chevron interface. The degree of this tilt comes from a complex interaction of all the smectic C thermodynamics forces. However, by looking at the relative sizes of the smectic C thermodynamic forces $(K/B)^{1/2}\ll 1$ [19] and $\gamma_\parallel q_A^2 \gg D_\perp q_A^4$ [20] we will be able to exploit the dominance of the layer dilatation energy to simplify the calculations. With dilatational energy minimized absolutely in the chevron, then out-of-plane director tilt α can be calculated explicitly for a symmetric chevron to be

$$\alpha_c \approx \pm(-2\varepsilon)^{\frac{1}{2}}. \tag{12}$$

Thus negative strain is necessary to produce symmetry breaking at the chevron tip. We speculate that this negative layer strain occurs as a result of molecular pretilt at cell surfaces. There is strong supporting experimental evidence to confirm that this out-of-plane tilt, α_s, is very close to the surface pretilt [21]. Notice also that writing equation (11) in terms of α_c yields the relationship found by Rieker *et al.* [4], equation (3).

The smectic C cone angle θ_B can be identified in terms of the phenomenological parameters by substituting

equation (10) into (9 *a*), yielding the free energy for uniformly tilted layers, taking $W = q_A z$ and $\mathbf{n} = (\sin\theta_B, \cos\theta_B)$ and minimizing with respect to θ_B to yield [14]

$$\theta_B \approx \tan^{-1}\theta_B = \left(\frac{|\gamma_\perp|}{2Dq_A^2\eta_B^2}\right)^{1/2}. \tag{13}$$

We find it helpful at this point to use these preliminaries to re-write the equations in a more physically intuitive way. This is done by first obtaining an expression for the free energy of planar or uniformly tilted layers. Substituting for equation (10) into (9 *a*) yields

$$\begin{aligned} F_{\text{tilt}} = \int & -\gamma_\perp \eta^2 \left[(\nabla W_e)^2 - q_A^2\right] \\ & + D_\perp \eta^2 \left[(\nabla W)_e^2 - q_A^2\right]^2 \mathrm{d}^3\mathbf{r}. \end{aligned} \tag{14}$$

It is useful to define the free energy relative to that of the equilibrium tilted layers F_{tilt}. This allows the free energy to be written in a physically more intuitive way:

$$\Delta F = \mathcal{F} - \mathcal{F}_{\text{tilt}} = \int_V f_n + f_{\text{dil}} + f_{\text{cone}} + f_{\text{grad}}\, \mathrm{d}^3\mathbf{r}$$

where

$$f_n = \frac{1}{2}K\left[(\nabla\cdot\mathbf{n})^2 + \nabla\times\mathbf{n})^2\right] \tag{15 b}$$

$$f_{\text{dil}} = \frac{1}{2}\gamma_\parallel \eta_B^2 q_A^2 \left[\frac{1}{q_A^2}(\mathbf{n}\cdot\nabla W) - q_A\right]^2 \tag{15 c}$$

$$f_{\text{cone}} = \frac{1}{2}D_\perp \eta_B^2 q_A^4 \left[\frac{1}{q_A^2}\left\{(\nabla W)^2 - (\mathbf{n}\cdot\nabla W)^2\right\} - \tan^2\theta_B\right]^2 \tag{15 d}$$

$$f_{\text{grad}} = \frac{1}{2}D_\perp \left[\nabla_\perp^2 W\right]^2. \tag{15 e}$$

We have identified the smectic C cone angle θ_B using equations (13) and (10). The physical meaning of these quantities is as follows: f_n represents the usual Frank director distortions of a nematic LC; f_{dil} is the cost for dilating the layers away from their equilibrium thickness q_A; f_{cone} maintains the equilibrium cone angle θ_B with respect to layer rotations; f_{grad} records the free energy cost of layer curvature and is in addition required for maintaining layer continuity at the chevron interface.

3.2. *Chevron layer profile*

If we consider the smectic dilatation energy to be dominant and enforce zero layer dilatation, then the layer profile may be derived analytically. Zero dilatation, obtained by substituting equation (10) into (15), decouples **n** and W, allowing the free energy to be written as

$$\begin{aligned} \Delta F = \int_V & D_\perp \eta_B^2 q_A^4 \left[\frac{1}{q_A^2}\left\{(\nabla W)^2 - q_A^2\right\} - \tan^2\theta_B\right]^2 \\ & + \frac{1}{2}D_\perp \left[\nabla_\perp^2 W\right]^2. \end{aligned} \tag{16}$$

This system is invariant with respect to translation in the y-direction, in the cell plane, perpendicular to the layer normals. We can therefore substitute for the layer phase $W = q[z - u(x)]$, where $u(x)$ describes the layer profile. Rewriting the free energy in terms of angular variables $\delta \approx \mathrm{d}u(x)/\mathrm{d}x$ yields

$$\begin{aligned} \Delta F = \int & \frac{1}{2}D_\perp \eta_B^2 q_A^4 \left[\delta(x)^2 - \left(2\varepsilon + \theta_B^2\right)\right]^2 \\ & + \frac{1}{2}D_\perp \eta_B^2 q_A^2 \left[\frac{\mathrm{d}\delta(x)}{\mathrm{d}x}\right]^2. \end{aligned} \tag{17}$$

The layer profile is obtained by solving the corresponding Euler–Lagrange equation:

$$\delta(x) = \delta_B \tanh(\lambda_c x) \tag{18}$$

where $\delta_B^2 = 2\varepsilon + \theta_B^2$ and the chevron width is given by $\lambda_c = \delta_B q_A$. It is interesting to observe that $\delta_E^2 = 2\varepsilon + \theta_B^2$ is an angular geometric condition in the presence of constant layer width. It can be expressed in terms of out-of-plane director tilt at the tip centre by

$$\delta_B^2 \approx \theta_B^2 - \alpha_c^2. \tag{19}$$

This confirms that out-of-plane director tilt is indeed associated with a reduction in layer tilt. Again, this is the result observed by Rieker *et al.*, equation (3).

3.3. *Quasi-static switching energy*

We now calculate the surface switching energy in terms of the macroscopic chevron boundary angle ϕ_s. In principle, this requires one to consider the dynamic coupling between the rotation of the director and movement of the smectic layers during the switching process. Fortunately, we can neglect inertial switching and consider the process as quasi-static. We can further assume the layers to remain fixed during the switching process due to the relatively slow response of layer motion, occurring in the order of seconds [22], in comparison with the much faster director dynamics occurring on a time scale of the order 10^{-6} s [19].

The chevron interface will be considered in the following way. Away from the tip the far field mesoscopic boundary condition will be taken to be the discontinuous limit of the macroscopic continuum theory, as defined by equation (2). In this region we must have zero layer dilatation and so equation (10) can

be written as

$$q = \frac{q_A}{\delta_B n_x^e + n_z^e} \tag{20}$$

where n_x^e and n_z^e are determined by $n_x = 0$, δ_B and θ_B. Thus they also determine the angular variable $\phi_s = \phi_c$ at the chevron interface.

When we switch from one state to the other we will perturb the system away from this equilibrium state as we have fixed the layer structure. Thus moving the director away from its equilibrium is associated with energy costs from nematic curvature equation (15 *b*), layer dilatation (15 *c*) and cone angle maintenance costs (15 *d*). The greatest contributions to the free energy come from nematic curvature and smectic compression. If the cone angle variation costs are neglected, the free energy in equation (15 *a*) can be written as

$$F = \int \frac{1}{2} K \left[\left(\frac{\partial n_x}{\partial x} \right)^2 + \left(\frac{\partial n_y}{\partial x} \right)^2 + \left(\frac{\partial n_z}{\partial x} \right)^2 \right] + \gamma_{\|} \eta^2 q_0^2 \left[\frac{\delta(x) n_x + n_z}{\delta_B n_x^e + n_z^e} - 1 \right]^2 dx \tag{21}$$

where ∇W_e has been replaced by its angular equivalent δ_B, and q has been substituted by the far field equilibrium value, equation (20). This formulation is naturally constrained by $|\mathbf{n}| = 1$.

In order to calculate the surface tension we require the director path across the interface. On a macroscopic level the path is irrelevant. Only the cone intersection at the interface is necessary, as shown in figure 5 (*b*). By contrast, the mesoscopic regime requires the director path to be calculated. This is true even when the far field director orientation obeys the cone matching condition. The path is expected to follow the layer position closely (see for example path 1 shown in figure 5 (*b*)). To obtain such a path requires the minimization of the free energy with respect to **n** and is non-trivial. However, it will be sufficient to approximate satisfactorily using a simple approximation for the director path across the interface. This choice is path 2, greatly simplifying the calculation, while still providing a good estimate for the distortion energy in the interface region.

Path 2 allows only the x-component of the director to be free. The free energy in this case can now be written, in the small angle limit, as

$$F = (n_x^e)^2 \int \frac{1}{2} K \left(\frac{\partial \bar{n}_x}{\partial x} \right)^2 + B_{ch} \left[\bar{\delta} \bar{n}_x + 1 \right]^2 dx \tag{22}$$

where $B_{ch} = \eta^2 q_A^2 \left[\delta_B n_x^e \right]^2$.

In general, solutions to equation (22) can only be found numerically. However, the problem can be simplified by using the approximation $\bar{n}_x = -\bar{\delta}$. This

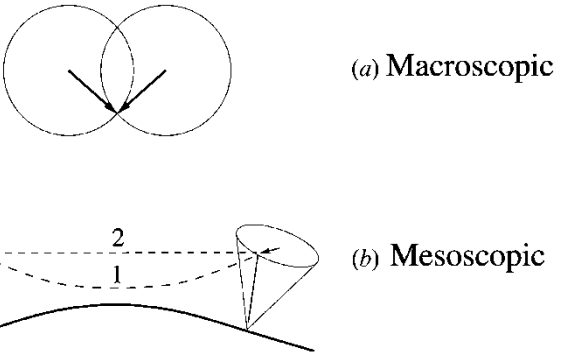

Figure 5. (*a*) Macroscopic picture illustrating the conditions governing director continuity at the chevron interface, as shown in figure 4. The two circles represent possible director orientations around the smectic C cone, consistent with each well-defined layer orientation. In this picture the chevron interface is thought of as infinitely thin. (*b*) Mesoscopic picture showing actual continuous director changes across the chevron interface. Path 1 indicates the (unknown) true path, and path 2 is a good approximation to this path. We use path 2 as an approximation of the true path. The director is not constant; it maintains its out-of-(layer)plane component, but its in-plane component can vary in response to layer orientation changes.

approximation also requires that $\lambda_n = \lambda_\delta$. The problem can now be written in standard Ginzburg–Landau form [23]

$$F = \int \frac{1}{2} K \left(\frac{\partial \bar{\delta}}{\partial x} \right)^2 + \bar{B} \left[\bar{\delta}^2 - 1 \right]^2 dx. \tag{23}$$

This has a standard minimizer, and the director profile n_x is given by:

$$n_x = n_x^E \tanh(x / \lambda_{n,\delta}) \tag{24}$$

where $\lambda = \left(K / B_c^- h \right)^{1/2} = q_A \delta_B$.

The corresponding free energy is:

$$F = \frac{4}{3} (K B_{ch})^{1/2} \delta_B \left(n_x^E \right)^2. \tag{25}$$

The minimum surface energy state is obtained when $n_x^E = 0$. This is simply the cone matching condition, which imposes director continuity at the chevron interface in the macroscopic continuum theory. There is a wholly analogous, although *ad hoc*, term in the theory of Maclennan *et al.* [7, 8].

The chevron interface energy can now be expressed in terms of the angular variables of the macroscopic continuum theory:

$$w(\phi_s) = \frac{8}{3\sqrt{2}} (K B_{ch})^{1/2} \delta_B \sin^2 \theta_B \cos^2 \delta_B (\cos \phi_s - \cos \phi_c)^2 \tag{26}$$

$$w(\phi_s) = w_c (\cos \phi_s - \cos \phi_c)^2 \tag{27}$$

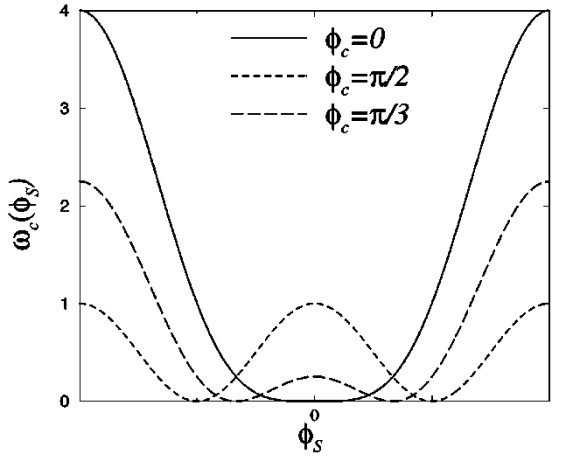

Figure 6. General chevron anchoring energy.

where we have identified ϕ_c using $n_x^E = 0$ as

$$\cos\phi_c = -\frac{\tan\delta_B}{\tan\theta_B} \tag{28}$$

and $w_c = \frac{4}{3}(KB_{ch})^{1/2}\delta_B \sin^2\theta_B \cos^2\delta_B$.

The general form of $w(\phi_s)$ can be seen in figure 6. The free energy landscape is determined by ϕ_c. When $\phi_c = 0$ or π there is only a single well and no bistability. In the case that $\phi_c \neq 0$ the free energy landscape takes a double-well shape, leading to bistability. The switching process attempts to move ϕ_s from one minimum to another. The energy cost of switching is dependent on which way ϕ_s takes from one minimum to another, as shown in the case where $\phi_c = \pi/3$. A special case exists when $\phi_c = \pi/2$ when rotation in either direction costs the same energy.

In the small ϕ angle limit the surface energy term becomes a simple double-well potential

$$w_c = \frac{1}{4}w_c\left(\phi_S^2 - \phi_c^2\right)^2. \tag{29}$$

This effective chevron surface anchoring energy can be calculated using typical ferroelectric material parameters [24] to be $\sim 5\times10^5\,\mathrm{J\,m^{-2}}$, which is the upper limit of surface anchoring energies.

In the next section we use this free energy in the presence of an imposed electric field to gain insight into likely switching scenarios. In § 5 we combine the free energy with an equation of motion to examine the details of the dynamics of the switching process.

4. Hybrid model: equilibrium considerations

In this section we elaborate our hybrid switching model introduced in § 2.6. This will combine the macroscopic smectic C continuum theory, § 2.4, equation (5), and the chevron surface energy calculation, § 3, equation (26). Rather than solving the full equation to determine equilibrium solutions, we will calculate an approximate set to allow us to concentrate on understanding the underlying physics of the switching process.

The free energy of the cell is obtained by combining the macroscopic distortion free energy, equation (5), and the surface energy condition (26). In order to simplify this free energy we apply the single B elastic approximation ($B = B_1 = B_2 = B_3$) with $B_{13} = 0$, to yield

$$F = \int_0^L \left[\frac{1}{2}B\phi_x^2 - P_\perp E_\perp \sin\phi\right]\mathrm{d}x + w_c(\cos\phi_s - \cos\phi_c)^2. \tag{30}$$

The quantities $P_\perp = P\sin\theta_B$ and $E_\perp = E\cos\delta_E$ are the projected components of P and E, and do not take their bare values as a result of layer tilt. The electric field term should determine the bulk orientation. In the absence of external constraints the equilibrium orientation of the director orients to $\phi_E = \pm\pi/2$, depending on the sign of E. However, the presence of the cell and chevron interfaces provides couples orienting the directors at $\phi(0) = \phi_0$ and $\phi(L) = \phi_c$. Finally, the gradient term prevents ϕ changing discontinuously between the two boundaries.

There are three length scales involved in this macroscopic system. These are: (i) the electric penetration depth ξ_e, (ii) the surface chevron surface extrapolation length λ_s, and (iii) the ferroelectric cell thickness divided by 2. These are defined respectively as:

$$\xi_e = \left(\frac{B}{|P_\perp E_\perp|}\right)^{1/2},\ \lambda_s = \frac{B}{w_c},\ L. \tag{31}$$

From these we can construct two independent dimensionless ratios, and the most convenient for our purpose will be: (a) the non-dimensional field strength $\hat{E} = L^2/\xi_e^2$; (b) the dimensionless cell size $\ell = L/\lambda_s$.

The Euler–Lagrange equations corresponding to equation (30) possess closed form solutions in terms of elliptic integrals [7]. However, we shall not make explicit use of these solutions, but rather we identify the point of absolute instability of the solution branch corresponding to a particular global orientation, where the instability is induced by the presence of the opposing electric field. For analytical tractability we concentrate on the physics close to the onset of switching where we expect E to be close to the switching threshold field E_{th} and $\phi(x) \ll \phi_E$. In this regime it is reasonable to expand the free energy in ϕ, yielding:

$$F = \int_0^L \mathrm{d}x\left[\frac{1}{2}B\phi_x^2 - P_\perp E_\perp\phi\right] + \frac{1}{4}w_c\left(\phi_s^2 - \phi_c^2\right)^2. \tag{32}$$

We note here that whereas only the first power of ϕ in the bulk term has been retained, in the surface term

the expansion is to fourth order. The bulk linear term in ϕ is not bounded. However the surface terms mean that the full functional is bounded, and the approximation is only valid when the small ϕ solution holds. Although this level of approximation is clearly inaccurate away from field and length critical points, it does yield useful information close to these points, providing a simple insight into the switching process.

4.1. *Azimuthal angular profile across the cell*

It is now useful to write the free energy, equation (32), in non-dimensional form as:

$$\bar{F} = \int_0^1 \left[\frac{1}{2}\phi_\rho^2 - \hat{E}\phi\right] \mathrm{d}\rho + \frac{\ell}{4}\left(\phi_s^2 - \phi_c^2\right)^2 \qquad (33)$$

with non-dimensional free energy $\bar{F} = F\frac{L}{B}$.

The corresponding Euler–Lagrange equation is:

$$\phi_{\rho\rho} = -\hat{E} \qquad (34)$$

subject to the boundary condition $\phi(0) = 0$ (for convenience) and the variational chevron surface condition:

$$\phi_{\rho|s} + \ell\phi_s\left(\phi_s^2 - \phi_c^2\right) = 0. \qquad (35)$$

Equation (34) can be solved by integrating twice and applying the boundary conditions $\phi(0) = 0$ and $\phi(1) = \phi_s$. This yields:

$$\phi(\rho) = -\frac{1}{2}\hat{E}\left(\rho^2 - \rho\right) + \phi_s\rho. \qquad (36)$$

To determine the equilibrium value of ϕ_s requires the simultaneous solution of equations (34) and (35). However, as we see below, it is more useful to calculate the free energy as a function of ϕ_s, and minimize this quantity.

4.2. *Equilibrium phase diagram and cone matching*

The stability regimes can be obtained from the solutions (34) and (35). We substitute equation (36) into (33); we then integrate (33) explicitly. This yields a free energy as a function of the chevron angle ϕ_S:

$$\bar{F} = \frac{1}{2}\phi_s^2 - \frac{1}{2}\hat{E}\phi_s - \frac{1}{24}\hat{E}^2 + \frac{1}{4}\ell\left(\phi_s^2 - \phi_c^2\right)^2 \qquad (37)$$

$$\bar{F} = -\frac{1}{2}\hat{E}\phi_s + \frac{1}{2}\left(1 - \ell\phi_c^2\right)\phi_s^2 + \frac{\ell}{4}\phi_s^4 + \ldots. \qquad (38)$$

where the dots indicate terms independent of ϕ_s.

Equation (38) is of the same form as the Landau theory of an Ising model with field variable ϕ_S, in a field $\hat{E}$, identifying ℓ with the temperature variable, and with $\ell\phi_c^2 < 1$ as the high temperature regime. The qualitative form of the solutions is thus given by considering the Ising model.

The solution structure is as follows.

(a) For $\ell\phi_c^2 < 1$, i.e. extremely thin cells, $\bar{F}$ has a single minimizer. For $\hat{E} = 0$, this occurs at $\phi_s = 0$, and at small $\hat{E}$,

$$\phi_s \approx \left(\frac{1}{1 - \ell\phi_c^2}\right)\frac{\hat{E}}{2}.$$

This corresponds to thresholdless switching of the cell. There is no hysteresis as a function of field, and the polarization will begin to switch toward the favoured direction even at infinitely low fields.

(b) At $\ell\phi_c^2 = 1$, there is a symmetry breaking transition and a critical point. Here, in the same limit

$$\phi_S = \left[\frac{1}{2}\hat{E}\ell^{-1}\right]^{1/3}.$$

(c) For $\ell\phi_c^2 > 1$, at zero $\hat{E}$, there are two energetically degenerate solutions $\phi_s(\ell) = \pm\left(\phi_c^2 - \ell^{-1}\right)^{1/2}$, corresponding to 'up' and 'down' states. The system is now bistable. As the cell becomes thicker, ϕ approaches the cone angle value ϕ_c at which there is director continuity at the chevron interface. At finite values of $\hat{E}$, these solutions lose their degeneracy, with one solution becoming metastable. For a sufficiently large value of $\hat{E}$, at the *spinodal* line, the metastable solution loses its local stability. This is the switching threshold line.

The spinodal condition is that both $\frac{\partial F}{\partial \phi_s} = 0$ and $\frac{\partial^2 F}{\partial \phi_s^2} = 0$. After some algebra, this yields for the threshold field:

$$\hat{E} = \frac{4}{3\sqrt{3}}\ell^{-1/2}\left(\ell\phi_c^2 - 1\right)^{3/2}. \qquad (39)$$

The resulting phase diagram is summarized in figure 7.

5. Switching dynamics

5.1. *Equations of motion*

In this section the dynamical equations that describe switching in the bulk and at the chevron surface are presented. As shown in the previous section it has been possible to write the macroscopic bulk free energy in terms of $\phi(x)$ and the mesoscopic chevron surface energy in terms of a single variable ϕ_S (equation (30)). In general form this is simply written as

$$F = \int_0^L f\left[x, \phi(x), \phi'(x)\right]\mathrm{d}x + w_c(\phi_s) \qquad (40)$$

where $f = f_B + f_E$ is the free energy density containing a bulk elastic and electric term and $w(\phi_s)$ is the surface

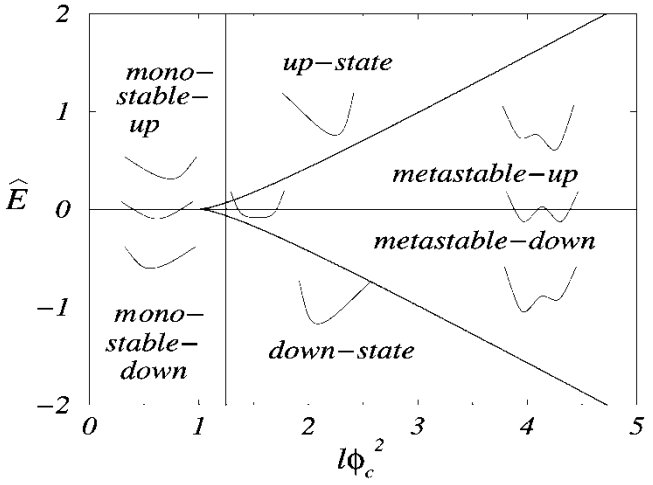

Figure 7. Equilibrium phase diagram governing cell switching properties, as a function of dimensionless parameter $\ell\phi_c^2$ and field $\hat{E}$. We have taken $\phi_c=\pi/4$ for diagrammatical convenience. Also shown: diagrams of free energy structure in each region.

chevron anchoring energy, where ϕ_s is the value of ϕ on the chevron surface.

We model the dynamics using coupled bulk and surface time-dependent Ginzburg–Landau equations:

$$\eta_B \frac{\partial\phi}{\partial t} = -\frac{\delta F}{\delta\phi} = -\left[\frac{\partial f}{\partial\phi} - \frac{\partial}{\partial x}\frac{\partial f}{\partial\phi_x}\right], \text{ Bulk} \qquad (41\,a)$$

$$\eta_s \frac{\partial\phi_s}{\partial t} = -\frac{\delta F}{\delta\phi}\bigg|_S = -\left[\frac{\partial f}{\partial\phi_x}\bigg|_s + \frac{\partial w}{\partial\phi_s}\right], \text{ Chevron surface,} \qquad (41\,b)$$

where η_B is the normal bulk relaxation of the chosen order parameter or just the relevant rotational Leslie viscosity coefficient; and η_s is a chevron surface viscosity. An exact evaluation of η_s is difficult. However, an estimate based on the chevron geometry should provide sensible physical bounds on its magnitude. This estimate yields $\eta_s \approx \lambda_c \eta_B$ where λ_c is a measure of the chevron tip width.

The dynamics can again be understood by simply substituting the approximate free energy equation (32) into (41 *a*) and (41 *b*), to yield

$$\tau_1 \frac{\partial\phi}{\partial t} = -\left(-\hat{E}\cos\phi - \phi_{\rho\rho}\right) \qquad (42\,a)$$

$$\tau_2 \frac{\partial\phi_s}{\partial t} = -\left(\phi_{s,\rho} - 2\ell\cos\phi_s - \cos\phi_c \sin\phi_s\right) \qquad (42\,b)$$

where we have used the scalings of the last section, defined in equation (31). For convenience, the time scales for the relaxation of the bulk τ_1 and the surface τ_2 are identified as:

$$\tau_1 = \frac{\eta_B L^2}{B_1},\ \tau_2 = \frac{\eta_s L}{B_1}. \qquad (43)$$

These are the most convenient time scales for numerical calculation purposes. They refer to the relaxation of the bulk in the absence of an electric field and the relaxation of the surface condition due to bulk distortions, respectively. However, they are not the true time scales for the field-induced switching process as determined by ferroelectric device parameters.† In the presence of a field and the bistable switching condition, the appropriate time scales for bulk and surface relaxation are determined by equating terms in equation (42 *a*) to be

$$\tau_B = \frac{\eta_B}{P_\perp E_\perp},\ \tau_S = \frac{\eta_s}{w_c}. \qquad (44)$$

For the device to switch to saturation one requires $\xi_e \ll L$ and $\lambda_s \ll L$. The second condition asserts that the chevron surface torques are balanced in a region λ_s close to the chevron tip. These conditions are both satisfied for standard ferroelectric materials. The ratios of the natural time scales for the dynamics of the switching process can now be determined. Rewriting them in terms of their corresponding length scales, we obtain

$$\frac{\tau_B}{\tau_S} = \frac{\eta_B}{P_\perp E_\perp}\frac{w}{\lambda_{ch}\eta_B} = \frac{\xi_e^2}{\lambda_{ch}\lambda_s}. \qquad (45)$$

Estimates of material parameters [24] set $\tau_B \sim 10^{-5}$ s and $\tau_S \sim 10^{-6}$ s. Thus the surface relaxes an order of magnitude faster than the bulk. The limiting time scale for switching involves bulk reorientation of the smectic cone rather than relaxation of the chevron interface. This result can also be obtained using standard methods of rational mechanics.‡

The full set of switching equations have been solved numerically (using standard methods [24]) in representative cases. We have calculated the time required for the surface condition ϕ_s to travel from the previously stable minimum to $\phi_s = 0$. This is the point at which the field may be removed to allow complete switching to the other minimum. We define this minimum time as τ_{min}, referred to as the latching time in the literature. These results of τ_{min} for varying field strengths can be seen in figure 8. The numerically calculated switch is shown for characteristic ferroelectric parameter values, while varying the electric field strength. We notice that the switching time τ_{min} follows closely the time scale for

†Typical ferroelectric liquid crystal parameters are $P = 300\times10^6\,\mathrm{C\,m^{-2}}$, $B = 10^6\,\mathrm{J\,m^{-3}}$, $K = 10^{-11}\,\mathrm{J\,m^{-1}}$, $\delta = 0.2$ rad, $\theta = 0.25$ rad, $B_i = 10^{-12}\,\mathrm{N}$, $L = 3\times10^{-6}\,\mathrm{m}$, $E = 10^7\,\mathrm{V\,m^{-1}}$, $\eta_B = 0.01\,\mathrm{kg\,m^{-1}\,s^{-1}}$.

‡Using a trial solution for $\phi(\rho)$ it is possible to obtain the free energy in terms of the bulk and surface contributions, i.e. $F[\phi_s] = F_B[\phi_s] + F_s[\phi_s]$. By relating this free energy through a dissipation function we may write $(\eta_B + \eta_B)\frac{\partial\phi_s}{\partial t} = -\frac{\partial F[\phi_s]}{\partial\phi_s}$. The limiting time scale for the relaxation is proportional to η_B, as $\eta_B \gg \eta_s$.

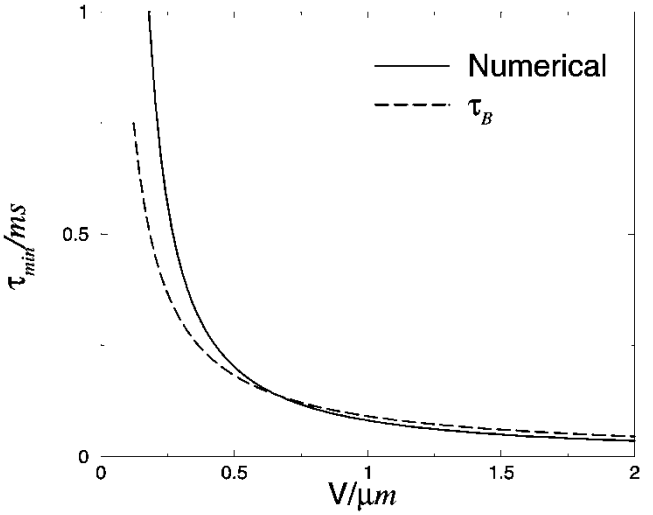

Figure 8. $\tau_{\min}$–V switching curve.

the bulk relaxation τ_B. For high fields the switching is limited by the chevron surface relaxation time scale τ_s. We should remind the reader that we have not included the contribution of dielectric anisotropy. If this had been included in the calculation then $\tau_{\min}$ would begin to increase again with field, as discussed, for example, by Sako *et al.* [25].

The $\phi(\rho)$ profile, taken at the latching point, is shown in figure 9. This shows characteristically different profiles for switching close to the switching threshold (curved), and those obtained for high fields (flattened). It is also clear that the switch occurs first at the cell surface and not at the chevron interface. However, this follows from our choice of anchoring at this boundary

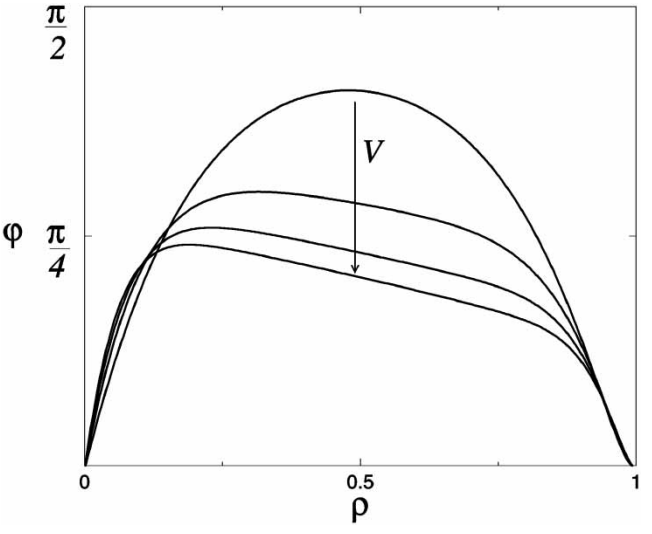

Figure 9. $\phi(\rho)$ at the latching point.

and would be pushed back to the chevron interface when surface anchoring strengths exceed the chevron surface interfacial energy.

6. Discussion and conclusions

The understanding of switching in ferroelectric smectic cells requires the use of unexpectedly complex theoretical models. This complexity is primarily due to the contrasting physics required for director switching, occurring over relatively large spatial scales, and the physics of the chevron structures often found within FLC devices, which involves very short range processes. Macroscopic continuum theory is the ideal tool for describing the switching process in the chevron arms, in which the director and the layer tilt vary slowly. However, this type of theory is by its very nature unable to describe the chevron interface region. By contrast, mesoscopic phenomenological theories are ideal for describing the interface region, but come at the price of working unrealistically hard in the slowly varying chevron arms. Previous workers have developed hybrid theories which combine macroscopic models with an *ad hoc* term to describe the chevron interface region.

In this paper we have replaced this *ad hoc* chevron term with one calculated explicitly using the phenomenological Landau–de Gennes smectic C chevron theory. We find that this naturally leads to the macroscopically defined chevron cone matching condition. When we include it in a macroscopic hybrid theory, we are now able to produce a detailed switching phase diagram close to switching thresholds. The theory now demonstrates physically the conditions required for thresholdless and bistable switching phenomena. In the dynamical case we have shown that the chevron surface relaxes quickly on the time scale required for bulk reorientation and that it is the bulk which restricts ferroelectric switching. This is consistent with experiment. Finally, a numerical solution of the switching process of the full equations is presented to confirm our analytical predictions.

The model presented in this paper does not yet develop a self-consistent treatment of the electric field and the contribution from dielectric components to the free energy. A full theory must include these effects. However, these extensions do not involve issues of principle. We are confident that the inclusion of these features will not affect the general structure of the switching phase diagram. Rather, it will be found that the switching threshold values and time scales will be rescaled.

Furthermore, the present treatment has considered only uniform switching in the cell, omitting the possible heterogeneous spatial nature of the switching process

involving domain formation. In principle, our methodology can be extended to include these features, although by necessity the resulting calculation will be considerably more complex.

This work was funded by DERA, Malvern, UK and we are grateful to members of the Liquid Crystal Group, particularly Cliff Jones, Carl Brown and Victor Hui for their contribution this work. We are also grateful to Colin Please for discussions concerning the numerical strategy adopted in solving some of the equations. We thank James Steele for encouragement.

References

[1] MEYER, R. B., LIEBERT, L., STRZELECKI, L., and KELLER, J., 1975, *J. Phys. Lett. (Paris)*, **36,** L69.
[2] CLARK, N. A., and LAGERWALL, S. T., 1980, *Appl. Phys. Lett.*, **36,** 899.
[3] HANDSCHY, M. A., and CLARK, N. A., 1984, *Ferroelectrics*, **59,** 69.
[4] RIEKER, T. P., CLARK, N. A., SMITH, G. S., PARMAR, D. S., SIROTA, E. B., and SAFINYA, C. R., 1987, *Phys. Rev. Lett.*, **59,** 2658.
[5] LESLIE, F. M., STEWART, I. W., and NAKAGAWA, M., 1991, *Mol. Cryst. liq. Cryst.*, **198,** 443.
[6] VAUPOTIČ, N., GRUBELNIK, V., and ČOPIČ, M., 2000, *Phys. Rev. E*, **62,** 2317.
[7] MACLENNAN, J. E., CLARK, N. A., HANDSCHY, M. A., and MEADOWS, M. R., 1990, *Liq. Cryst.*, **7,** 753.
[8] MACLENNAN, J. E., HANDSCHY, M. A., and CLARK, N. A., 1990, *Liq. Cryst.*, **7,** 787.
[9] ULRICH, D. C., 1995, PhD Thesis, Oxford University, U.K.
[10] BROWN, C. V., DUNN, P. E., and JONES, J. C., 1997, *Eur. J. appl. Math.*, **8,** 281.
[11] DE MEYERE, A., and DAHL, I., 1994, *Liq. Cryst.*, **17,** 397.
[12] LIMAT, L., and PROST, J., 1993, *Liq. Cryst.*, **13,** 101.
[13] KRALJ, S., and SLUCKIN, T. J., 1994, *Phys. Rev. E*, **50,** 2940.
[14] VAUPOTIČ, N., KRALJ, S., ČOPIČ, M., and SLUCKIN, T. J., 1996, *Phys. Rev. E*, **54,** 3783.
[15] CLARK, N. A., and RIEKER, T. P., 1988, *Phys. Rev. A*, **37,** 1053.
[16] NAKAGAWA, M., 1992, *J. phys. Soc. Jpn.*, **61,** 4390.
[17] SABATER, J., PENA, J. M. S., and OTON, J. M., 1995, *J. Appl. Phys.*, **77,** 3023.
[18] CHEN, J.-H., and LUBENSKY, T. C., 1976, *Phys. Rev. A*, **14,** 1202.
[19] DE GENNES, P. G., and PROST, J., 1993, *The Physics of Liquid Crystals*, 2nd Edn, (New York: Oxford University Press).
[20] MARTINEZ-MIRANDA, L. J., KORTAN, A. R., and BIRGENEAU, R. J., 1986, *Phys. Rev. Lett.*, **56,** 2264.
[21] KANBE, J., INOUE, H., MIZUTOME, A., HANYUU, Y., KATAGIRI, K., and YOSHIHARA, S., 1991, *Ferroelectrics*, **114,** 3.
[22] MORSE, A. S., GLEESON, H. F., and CUMMINGS, S., 1997, *Liq. Cryst.*, **23,** 717.
[23] CHAIKIN, P. M., and LUBENSKY, T. C., 1995, *Principles of Condensed Matter Physics* (Cambridge: University Press).
[24] PRESS, W. H., TEUKOLSKY, S. A., VETTERLING, W. T., and FLANNERY, B. P., 1992, *Numerical Recipes in Fortran*, 2nd Edn, (Cambridge University Press).
[25] SAKO, T., ITOH, N., SAKAIGAWA, A., and KODEN, M., 1997, *Appl. Phys. Lett.*, **71,** 461.